MoS_2/Mn-Zn Ferrite Composite: An Enhanced Absorber for Excellent Microwave Absorption Performances

Xiaoyu Lin, Jing Wang*, Haozhi Liu and Qing Li
College of Liberal Arts and Sciences, National University of Defense Technology, Changsha, Hunan, China

These authors contributed equally to this work.

Keywords: MoS_2, Mn-Zn ferrite, Microwave absorption performance, Mechanism

Abstract: In this study, MoS_2/Mn-Zn ferrite composites were obtained by mixing MoS_2 and Mn-Zn ferrite via high-speed vibrating ball milling. The dielectric properties, magnetic properties and microwave absorption performance of MoS_2, Mn-Zn ferrite and their composites were investigated in the frequency of 2-18 GHz. Then the mechanism of electromagnetic loss was further explored. Our results show that the imaginary permittivity (ε'') and imaginary permeability (μ'') of MoS_2/Mn-Zn ferrite composites are between those of their parents, indicating that the composites have both dielectric and magnetic loss. The absorption capability of the composites is better than that of MoS_2 at low frequency, and at high frequency, it is better than that of Mn-Zn ferrite. Compared with their parents, the composites have thinner matching thicknesses and broader effective bandwidths without obviously affecting the minimum reflection loss (RL) (still between −50 dB to −60 dB). The broadest effective bandwidth is 3.43 GHz of MS-DMR40-2-1, and the thinnest matching thickness is 1.59 mm of MS-DMR40-1-2. The enhanced microwave absorption performances of MoS_2/Mn-Zn ferrite composites are mainly attributed to the improved impedance matching and dual-loss mechanism. We believe that MoS_2/Mn-Zn ferrite composites are promising for the potential applications as novel, efficient microwave absorbents.

1 INTRODUCTION

With the development of modern technology, more and more electronic products have entered people's lives, bringing convenience to people while causing electromagnetic pollution. Compared with water pollution, air pollution and soil pollution, electromagnetic pollution is invisible and unsmellable, but it affects everyone all the time. Therefore, developing novel, efficient microwave absorption materials has always been a hot spot in the field of materials and environmental protection.

In recent years, MoS_2 is an emerging two-dimensional material that has attracted significant attentions. (Novoselov et al., 2005) prepared the single- or few-layer MoS_2 by using mechanical cleavage, and these sheets exhibited high crystal quality. Then liquid exfoliation method was used to improve the preparation efficiency and yield (Coleman et al., 2011), this method is simple but the appearance of product is single. Hydrothermal method can be used to synthesize MoS_2-based composites with different morphologies (Ding et al., 2016) and phases (Li et al., 2017), which is beneficial for performance improvement. But the lateral size of the MoS_2 films obtained by the aforementioned methods is often on the order of several micrometers (Lee, 2012). Lee et al (2012) obtained large-area MoS_2 films on SiO_2/Si substrates with chemical vapor deposition (CVD). This method can produce large-area films with controllable thickness and high crystallinity.

Because of diverse preparation methods and unique physicochemical properties, MoS_2 has widely applications in lubrication (Chhowalla and Amaratunga, 2000), semiconductor (Radisavljevic et al., 2011), catalysis (Jaramillo et al., 2007; Zhang et al., 2017) and energy storage (Wang et al., 2015). In addition, the large specific surface area and high dielectric constant make it an excellent microwave absorption material (Ning et al., 2015). (Liang et al., 2016) investigated the microwave absorbing performance of two-dimensional MoS_2 nanosheets synthesized by hydrothermal method. The minimum reflection loss (RL) was −47.8 dB and the effective bandwidth was up to 4.5 GHz (11-15.5 GHz) with the

Lin, X., Wang, J., Liu, H. and Li, Q.
MoS2/Mn-Zn Ferrite Composite: An Enhanced Absorber for Excellent Microwave Absorption Performances.
DOI: 10.5220/0008186200970102
In *The Second International Conference on Materials Chemistry and Environmental Protection (MEEP 2018)*, pages 97-102
ISBN: 978-989-758-360-5

thickness of 2.4 mm. Hierarchical MoS_2 nanospheres compounded with polyvinylidene fluoride (PVDF) was designed by (Zhang et al., 2016), and this material showed an adjustable and improved performance in a wide frequency of 2-40 GHz. However, when MoS_2 is used independently, it will suffer from poor impedance matching, which will attenuate the absorption capability. Therefore, many studies have focused on improving impedance matching characteristics, and compositing with magnetic materials is an important method to achieve this goal (Wang et al., 2018).

Like carbonyl iron powder (CIP), ferrite is also a widely used magnetic material, especially Mn-Zn ferrite, with high magnetic permeability (Jiang et al., 2012) and high Curie temperature (Ahmed et al., 2015).(You et al., 2015) found that pre-sintered Mn-Zn ferrite had poor absorbing performance, and the minimum RL could only reached −2.9 dB, while the performance was significantly improved after annealing in H_2 atmosphere. The minimum RL at 13.6 GHz was −47.6 dB with the matching thickness of 1.85 mm. Obviously, this step increased the complexity and the cost.

For these reasons, we proposed to combine MoS_2 with Mn-Zn ferrite, and the results showed that the composites had inherited the advantages of their parents, improved impedance matching and better absorbing performance. They were promising for the potential applications as novel, efficient microwave absorbents, and the study of mechanism was very meaningful for the design of microwave absorbing materials.

2 EXPERIMENTAL SECTION

2.1 Materials

The commercial MoS_2 powder with purity of 99% was purchased from Macklin. Mn-Zn ferrite, number DMR40, was purchased from DongCiCo., Ltd. All reagents were used as received without further purification or grind.

2.2 Preparation of MoS_2/Mn-Zn Ferrite Composites and Coaxial Ring Samples

The composites were obtained by mixing commercial MoS_2 and Mn-Zn ferrite at a certain mass ratio by high-speed vibrating ball milling (NJ1-QM-3A, Midwest Co. Ltd, Beijing). The vibration time was 5min with grinding ball. After that, the paraffin and composite were weighed to achieve a mass ratio of 1:4. The paraffin was then melted at 80°C, and the composite was added to the melted paraffin for mixing. The paraffin solidified after heating was terminated. A special mold was then used to prepare coaxial ring samples with an inner diameter of 3 mm, an outer diameter of 7 mm and a thickness of 2-4 mm. The coaxial ring samples of MoS_2 and Mn-Zn ferrite were prepared in the same way without the vibration step.

2.3 Characterization

X-ray diffraction (XRD) patterns were recorded by using a Rigaku TTRⅢ X-ray diffractometer with Cu Kα radiation. Scanning electron microscopy (SEM) images were obtained using a VEGA 3 SBH. A vector network analyzer (VNA, Agilent, 8720ET) was used to measure electromagnetic properties. The testing frequency range was 2-18 GHz.

3 RESULTS AND DISCUSSION

3.1 Morphology and Structure

MoS_2 and Mn-Zn ferrite are pure components, and MS-DMR40-2-1 represents that the mass ratio of MoS_2 to Mn-Zn ferrite in the composite is 2:1. The same notation applies to other composites.

The XRD images of MoS_2, Mn-Zn ferrite and their composite (MS-DMR40-1-1) are shown in Figure 1(a). We can find that the main diffraction peaks of MoS_2 are well indexed to hexagonal MoS_2(JCPDS 77-1716), and the main diffraction peaks of Mn-Zn ferrite are well indexed to $Mn_{0.6}Zn_{0.4}Fe_2O_4$ (JCPDS 74-2401). The XRD image of MS-DMR40-1-1 is the superposition of MoS_2 and Mn-Zn ferrite.

The SEM images of MoS_2, Mn-Zn ferrite and their composite are shown in Figure 1(b)-(d). Small flakes with layer-structure can be observed in MoS_2, and many polygonal blocks can be observed in Mn-Zn ferrite. Owing to the high-speed vibrating ball milling process, the composite consist of thinner MoS_2 flakes and compressed ferrite polygonal blocks.

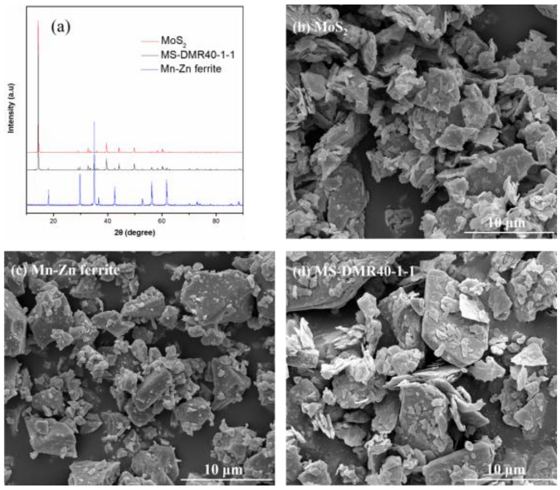

Figure 1: Characterization of MoS_2, Mn-Zn ferrite and MoS_2/Mn-Zn ferrite composite, XRD image (a); SEM images of (b) MoS_2, (c) Mn-Zn ferrite, (d) MS-DMR40-1-1.

3.2 Dielectric and Magnetic Properties

The real part (ε') and the imaginary part (ε'') of the complex permittivity ($\varepsilon_r=\varepsilon'-j\varepsilon''$) of MoS_2, Mn-Zn ferrite and MoS_2/Mn-Zn ferrite composties are shown in Figure 2. The ε' of the Mn-Zn ferrite is almost a constant in 2-14 GHz and fluctuates slightly in 14-18 GHz. The ε' of MoS_2 decreases with increasing frequency, and two inconspicuous relaxtion peaks appear at the mid-high frequency, corresponding to 10.2 and 14.6 GHz, respectively; the ε' of composites decreases with increasing frequency with multiple relaxtion peaks at high frequency, and exhibits a remarkable dispersion effect like that of MoS_2, which can be explained by the formula (1).

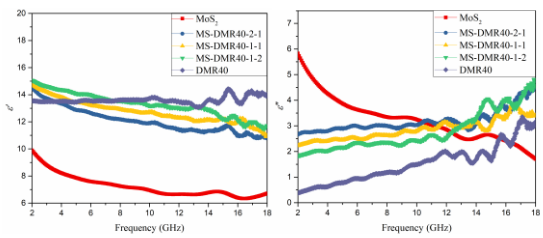

Figure 2: The complex permittivity of MoS_2, Mn-Zn ferrite and MoS_2/Mn-Zn ferrite composites.

In general, the dielectric loss can be expressed by the Debye theory as follows (Cao et al., 2012):

$$\varepsilon' = \varepsilon_\infty + \frac{\varepsilon_s-\varepsilon_\infty}{1+\omega^2\tau^2} \tag{1}$$

$$\varepsilon'' = \frac{\varepsilon_s-\varepsilon_\infty}{1+\omega^2\tau^2}\omega\tau + \frac{\sigma}{\omega\varepsilon_0} \tag{2}$$

Where σ is the dc conductive, ω is the angular frequency, τ is the polarization relaxation time, ε_s is the static permittivity, and ε_∞ is the relative dielectric permittivity at the high frequency limit.

According to the above two equations, the relationship between ε' and ε'' can be deduced as follows:

$$\left(\varepsilon' - \frac{\varepsilon_s+\varepsilon_\infty}{2}\right)^2 + \left(\varepsilon''^2\right) = \left(\frac{\varepsilon_s-\varepsilon_\infty}{2}\right)^2 \tag{3}$$

Thus, the curve of ε' versus ε'' is a single semicircle, which is called Cole-Cole semicircle, and each semicircle corresponds to a Debye relaxation process. As shown in Figure 3, two distinct semicircles can be observed in MoS_2, corresponding to two resonance peaks appearing at 10.2 and 14.6 GHz, indicating the dual-dielectric relaxation process. The composites have many segments of semicircles, corresponding to the resonance peaks appearing at high frequency, indicating the multi-dielectric relaxation process.

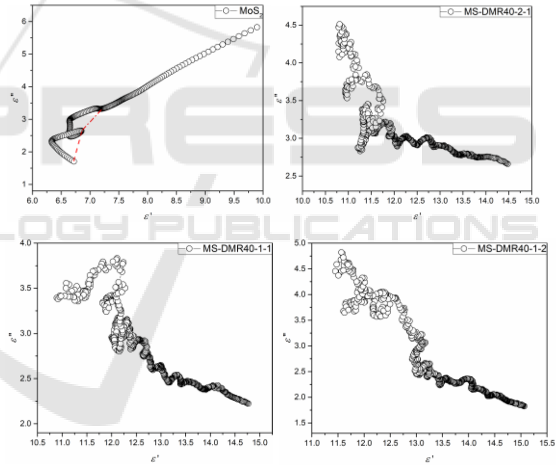

Figure 3: The Cole-Cole semicircle of MoS_2 and MoS_2/Mn-Zn ferrite composties.

The real part (μ') and the imaginary part (μ'') of the complex permeability ($\mu_r=\mu'-j\mu''$) of MoS_2, Mn-Zn ferrite and MoS_2/Mn-Zn ferrite composties are shown in Figure 4. The μ' of MoS_2 is floating around 1.1 modestly, while the μ' of the Mn-Zn ferrite and composites exhibits the same trend, first decreasing and then increasing with increasing frequency. The μ'' of MoS_2 is almost 0, while the μ'' of Mn-Zn ferrite and composites decreases with increasing frequency and drops to 0 at around 15 GHz, indicating that the magnetic loss is significant degraded.

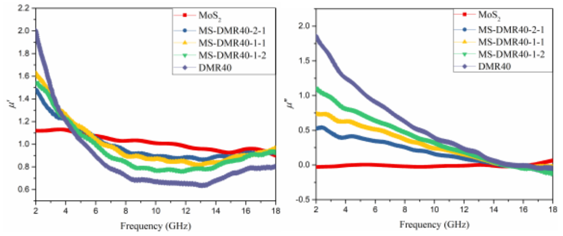

Figure 4: The complex permeability of MoS_2, Mn-Zn ferrite and MoS_2/Mn-Zn ferrite composties.

Generally, the magnetic loss is originated from hysteresis loss, domain-well resonance, eddy current effect and natural resonance. The hysteresis loss originating from the irreversible magnetization is negligible in a weak field (Wu et al., 2002), and the domain-well resonance usually appears in 1-100 MHz (Lu et al., 2008), so these two mechanisms can be excluded. Therefore, eddy current effect and natural resonance may be the main causes of magnetic loss.

The eddy current effect can be calculated from the skin-effect criterion. If $C_0=\mu''(\mu')^{-2}f^{-1}$ does not change with frequency, it means that the magnetic loss in this frequency range is originated from the eddy current effect (Liu et al., 2015). As shown in Figure 5, the C_0 values of the composites are almost a constant. Therefore, the magnetic loss of Mn-Zn ferrite is mainly caused by natural resonance, while the magnetic loss of the composites is mainly caused by natural resonance and eddy current effect.

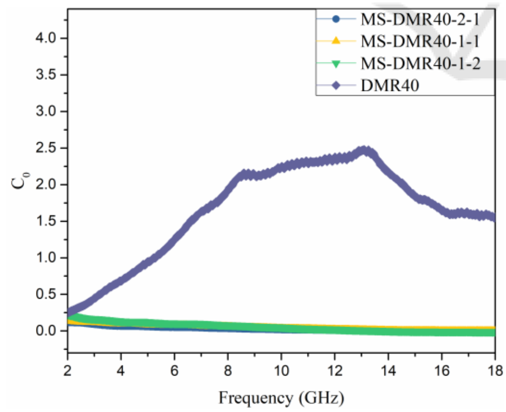

Figure 5: The C_0 values of Mn-Zn ferrite and MoS_2/Mn-Zn ferrite composties.

The dielectric tangent loss ($\tan\delta_\varepsilon$), magnetic loss tangent ($\tan\delta_\mu$) and dissipation factor ($\tan\delta=\tan\delta_\varepsilon + \tan\delta_\mu$) are shown in Figure 6. It is proved that MoS_2 is mainly dielectric loss material due to the fact that its $\tan\delta_\varepsilon$ is much larger than its $\tan\delta_\mu$. Although many researches categorize ferrite as dielectric and magnetic loss material, our results show that Mn-Zn ferrite is mainly magnetic loss material due to the fact that its $\tan\delta_\mu$ is much larger than its $\tan\delta_\varepsilon$. Figure 6 shows considerably large $\tan\delta_\varepsilon$ and $\tan\delta_\mu$ of the composites, indicating a dual-loss mechanism. The composites not only improve the microwave absorption capability of the MoS_2 at low frequency, but also improve the microwave absorption capability of Mn-Zn ferrite at high frequency.

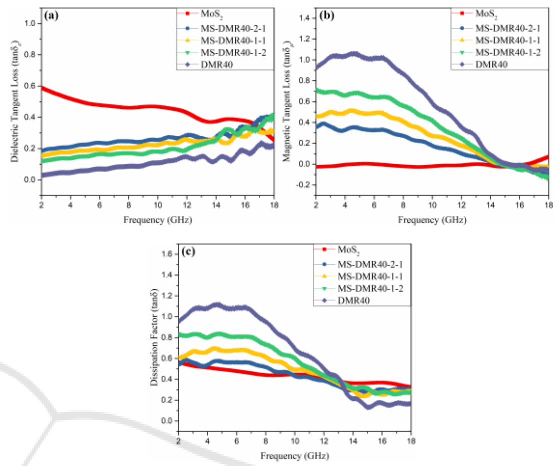

Figure 6: The (a) dielectric loss tangent, (b) magnetic loss tangent and (c) dissipation factor of MoS_2, Mn-Zn ferrite and MoS_2/Mn-Zn ferrite composties.

3.3 Microwave Absorption Performance

According to the transmission line theory, for single-layer microwave absorbents coated with metal backing, the RL values can be calculated from the measured electromagnetic parameters of coaxial ring samples at a given thickness and frequency:

$$RL(dB)=20\lg\left|\frac{Z_{in}-Z_0}{Z_{in}+Z_0}\right| \quad (4)$$

where Z_0 is the impedance of air, Z_{in} is the input impedance, which can be expressed as

$$Z_{in}=Z_0\sqrt{\frac{\mu_r}{\varepsilon_r}}\tanh\left[j\frac{2\pi fd}{c}\sqrt{\mu_r\varepsilon_r}\right] \quad (5)$$

where ε_r and μ_r are the complex permittivity and permeability of the absorbent, respectively, f is the frequency of incident electromagnetic wave, d is the thickness of the absorber and c is the velocity of light in free space.

We compare microwave absorption performance of MoS_2, Mn-Zn ferrite and MoS_2/Mn-Zn ferrite composites. As shown in Table 1 and Figure 7, the minimum RL of MoS_2 is −62.5 dB at 7.12 GHz with the matching thickness of 3.90 mm, and the effective bandwidth is 2.72 GHz (<−10 dB). The minimum RL of Mn-Zn ferrite is −42.7 dB at 13.48 GHz with the matching thickness of 1.91 mm, and the effective bandwidth is 2.35 GHz (<−10 dB). We can find that MoS_2 is dominant in getting higher RL, while Mn-Zn ferrite is dominant in getting thinner matching thickness. So, we propose that combining these two materials will result in a more optimized absorber. The effective bandwidths of the composites increase significantly, which are wider than those of their parents. The effective bandwidth of MS-DMR40-2-1 is up to 3.43 GHz. The matching thicknesses of the composites are thinner or at least equal than those of their parents. The matching thickness of MS-DMR40-1-2 is decreased to 1.59 mm, indicating that the impedance matching is improved. However, in order to achieve the effect of impedance matching, we scarify the microwave absorption capability. That is to say, although the magnetic permeability of the composites increases, the dielectric permittivity decreases. The increase in magnetic loss can not compensate for the decrease in dielectric loss. Meanwhile, it should be recognized that when the RL is below −10 dB, 90% of the microwave has been attenuated, and the improvement in effective bandwidth and matching thickness is more meaningful than increasing the minmum RL value. So, we think that the composites perform better than MoS_2 and Mn-Zn ferrite, and the development of the composites is very meaningful for practical applications.

Table 1: Microwave absorption performance of MoS_2, Mn-Zn ferrite and MoS_2/Mn-Zn ferrite composites.

Sample	Effective bandwidth /GHz	RL /dB	Matching thickness /mm
MoS_2	2.72	−62.50	3.90
MS-DMR40-2-1	3.43	−51.12	1.91
MS-DMR40-1-1	3.22	−50.75	1.80
MS-DMR40-1-2	3.15	−59.03	1.59
Mn-Zn ferrite (DMR40)	2.35	−42.76	1.91

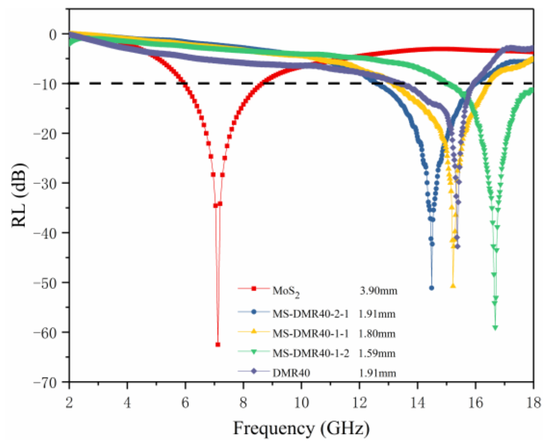

Figure 7: The theoretical RL curves of MoS_2, Mn-Zn ferrite and MoS_2/Mn-Zn ferrite.

4 CONCLUSIONS

In summary, we designed MoS_2/Mn-Zn ferrite composites by high-speed vibrating ball milling, and studied their electromagnetic performance. MoS_2 had the largest ε'' value and smallest μ'' value, while Mn-Zn ferrite was the opposite. The ε'' and μ'' of the composites were between those of MoS_2 and Mn-Zn ferrite, which meant a dual-loss mechanism in these absorbers. According to Debye theory, MoS_2 had a dual-dielectric relaxation process, while composites had a multi-dielectric relaxation process. According to the analysis of magnetic loss mechanism, the magnetic loss of Mn-Zn ferrite was mainly caused by natural resonance, while the magnetic loss of the composites was mainly caused by natural resonance and eddy current effect. We conclued that the improved performance of composites were mainly attibuted to the following three points: (1) the composites have both dielectric and magnetic loss; (2)the better impedance matching characteristics; (3) synergistic effect of MoS_2 and Mn-Zn ferrite.

This paper not only obtains microwave absorption materials with excellent performance, but also explores electromagnetic loss mechanism. We anticipate that our study could provide reference for the design and theoretical analysis of absorbing materials.

ACKNOWLEDGEMENTS

The work was financially supported by the National Natural Science Foundation of China (Grant No. 21403298) and the China Specialized Research Fund for the Doctoral Program of Higher Education (Grant No. 20134307120015).

REFERENCES

Ahmed, M.A., Rady, K.E. and Shams, M.S., 2015. “Enhancement of electric and magnetic properties of Mn-Zn ferrite by Ni-Ti ions substitution”, *Journal of Alloys and Compounds*, Vol. 622, pp. 269-75.

Cao, M.S., Yang, J., Song, W.L., Zhang, D.Q., Wen, B., Jin, H.B. Hou, Z.L. and Yuan, J., 2012. “Ferroferric Oxide/Multiwalled Carbon Nanotube vs Polyaniline/Ferroferric Oxide/Multiwalled Carbon Nanotube Multiheterostructures for Highly Effective Microwave Absorption”, *ACS Applied Materials & Interfaces*, Vol. 4 No. 12, pp. 6948-55.

Chhowalla, M. and Amaratunga, G.A.J., 2000. “Thin films of fullerene-like MoS_2 nanoparticles with ultra-low friction and wear”, *Nature*, Vol. 407 No. 6801, pp. 164-7.

Coleman, J.N., Lotya, M., O'Neill, A., Bergin, S.D., King, P.J., Khan, U., Young, K., Gaucher, A., De, S., Smith, R.J., Shvets, I.V., Arora, S.K., Stanton, G., Kim, H.Y., Lee, K., Kim, G.T., Duesberg, G.S., Hallam, T., Boland, J.J., Wang, J.J., Donegan, J.F., Grunlan, J.C., Moriarty, G., Shmeliov, A., Nicholls, R.J., Perkins, J.M., Grieveson, E.M., Theuwissen, K., McComb, D.W., Nellist, P.D. and Nicolosi, V., 2011. “Two-Dimensional Nanosheets Produced by Liquid Exfoliation of Layered Materials”, *Science*, Vol. 331 No. 6017, pp. 568-71.

Ding, X., Huang, Y., Li, S.P., Zhang, N. and Wang, J.G., 2016. “3D architecture reduced graphene oxide-MoS_2 composite: Preparation and excellent electromagnetic wave absorption performance”, *Composites Part A: Applied Science and Manufacturing*, Vol. 90, pp. 424-32.

Jaramillo, T.F., Jørgensen, K.P., Bonde, J., Nielsen, J.H., Horch, S. and Chorkendorff, I.. 2007. “Identification of Active Edge Sites for Electrochemical H_2 Evolution from MoS_2 Nanocatalysts”, *Science*, Vol. 317 No. 5834, pp. 100.

Jiang, K.Q., Li, K.K., Peng, C.H. and Zhu, Y., 2012. “Effect of multi-additives on the microstructure and magnetic properties of high permeability Mn-Zn ferrite”, *Journal of Alloys and Compounds*, Vol. 541, pp. 472-76.

Li, H.Y., Chen, S.M.; Jia, X.F., Xu, B., Lin, H.F., Yang, H.Z., Song, L. and Wang, X., 2017. “Amorphous nickel-cobalt complexes hybridized with 1T-phase molybdenum disulfied via hydrazine-induced phase transformation for water splitting”, *Nat. Commun*, Vol. 8, pp. 15377.

Liang, X.H., Zhang, X.M., Liu, W., Tang, D.M., Zhang, B.S. and Ji, G.B., 2016. “A simple hydrothermal process to grow MoS_2 nanosheets with excellent dielectric loss and microwave absorption performance”, *Journal of Materials Chemistry C*, Vol. 4 No. 28, pp. 6816-21.

Liu, P.B., Huang, Y. and Zhang, X., 2015. “Cubic $NiFe_2O_4$ particles on graphene–polyaniline and their enhanced microwave absorption properties”, *Composites Science and Technology*, Vol. 107, pp. 54-60.

Lu, B., Huang, H., Dong, X.L., Zhang, X.F., Lei, J.P., Sun, J.P. and Dong, C., 2008. “Influence of alloy components on electromagnetic characteristics of core/shell-type Fe–Ni nanoparticles”, *Journal of Applied* Physics, Vol. 104 No. 11, pp. 114313.

Ning, M.Q., Lu, M.M., Li, J.B., Chen, Z., Dou, Y.K., Wang, C.Z., Rehman, F., Cao, M.S. and Jin. H.B., 2015. “Two-dimensional nanosheets of MoS_2: a promising material with high dielectric properties and microwave absorption performance”, *Nanoscale*, Vol. 7 No. 38, pp. 15734-40.

Novoselov, K.S., Jiang, D., Schedin, F., Booth, T.J., Khotkevich, V.V., Morozov, S.V. and Geim, A.K., 2005. “Two-dimensional atomic crystals”, *PNAS*, Vol. 102 No. 30, pp. 10451-53.

Radisavljevic, B., Radenovic, A., Brivio, J., Giacometti, V. and Kis, A., 2011. “Single-layer MoS_2 transistors”, *Nature Nanotechnology*, Vol. 6, pp. 147-150.

Wang, J., Lin X.Y., Zhang R.X., Chu Z.Y. and Huang, Z.Y., 2018. “Transition metal dichalcogenides MX_2 (M=Mo, W; X=S, Se, Te) and MX_2-CIP composites: Promising materials with high microwave absorption performance”, *Journal of Alloys and Compounds*, Vol. 743, pp. 26-35.

Wang, J., Wu, Z.C., Hu, K.H., Chen, X.Y. and Yin, H.B., 2015. “High conductivity graphene-like MoS_2/polyaniline nanocomposites and its application in supercapacitor”, *Journal of Alloys and Compounds*, Vol. 619, pp. 38-43.

Wu, M.Z., Zhang, Y.D., Hui, S., Xiao, T.D., Ge, S.H., Hines, W.A., Budnick, J.I. and Taylor, G.W., 2002. “Microwave magnetic properties of $Co_{50}/(SiO_2)_{50}$ nanoparticles”, *Applied Physics Letters*, Vol. 80 No 23, pp. 4404-06.

You, C.Y., Fan, X.D., Tian, N. and He, J., 2015. “Good electromagnetic microwave absorption of the annealed pre-sintered precursor of Mn–Zn ferrite”, *Journal of Magnetism and Magnetic Materials*, Vol. 381, pp. 377-81.

Zhang, C.Y., Liu, B.N., Wang, Y.X., Zhao, L., Zhang, J., Zong, Q.Y., Gao, J.S. and Xu, C.M., 2017. “The effect of cobalt promoter on the CO methanation reaction over MoS_2 catalyst: a density functional study”, *RSC Advances*, Vol. 7 No. 20, pp. 11862-71.

Zhang, X.J., Li, S., Wang, S.W., Yin, Z.J., Zhu, J.Q., Guo, A.P., Wang, G.S., Yin, P.G. and Guo, L., 2016. “Self-Supported Construction of Three-Dimensional MoS_2 Hierarchical Nanospheres with Tunable High-Performance Microwave Absorption in Broadband”, *Journal of Physical* Chemistry *C*, Vol. 120 No. 38, pp. 22019-27.